J Biol Inorg Chem (2006) 11: 334–342
DOI 10.1007/s00775-006-0082-0

ORIGINAL PAPER

**Walleska De Jesús-Bonilla · Anthony Cruz
Ariel Lewis · José Cerda · Daniel E. Bacelo
Carmen L. Cadilla · Juan López-Garriga**

Hydrogen-bonding conformations of tyrosine B10 tailor the hemeprotein reactivity of ferryl species

Received: 17 October 2005 / Accepted: 16 January 2006 / Published online: 9 February 2006

Abstract Ferryl compounds [Fe(IV) = O] in living organisms play an essential role in the radical catalytic cycle and degradation processes of hemeproteins. We studied the reactions between H_2O_2 and hemoglobin II (HbII) (GlnE7, TyrB10, PheCD1, PheE11), recombinant hemoglobin I (HbI) (GlnE7, PheB10, PheCD1, PheE11), and the HbI PheB10Tyr mutant of *L. pectinata*. We found that the tyrosine residue in the B10 position tailors, in two very distinct ways, the reactivity of the ferryl species, compounds I and II. First, increasing the reaction pH from 4.86 to 7.50, and then to 11.2, caused the the second-order rate constant for HbII to decrease from 141.60 to 77.78 M^{-1} s^{-1}, and to 2.96 M^{-1} s^{-1}, respectively. This pH dependence is associated with the disruption of the heme–tyrosine (603 nm) protein moiety, which controls the access of the H_2O_2 to the hemeprotein active center, thus regulating the formation of the ferryl species. Second, the presence of compound I was evident in the UV–vis spectra (648-nm band) in the reactions of HbI and recombinant HbI with H_2O_2, This band, however, is completely absent in the analogous reaction with HbII and the HbI PheB10Tyr mutant. Therefore, the existence of a hydrogen-bonding network between the heme pocket amino acids (i.e., TyrB10) and the ferryl compound I created a path much faster than 3.0×10^{-2} s^{-1} for the decay of compound I to compound II. Furthermore, the decay of the heme ferryl compound I to compound II was independent of the proximal HisF8 *trans*-ligand strength. Thus, the pH dependence of the heme–tyrosine moiety complex determined the overall reaction rate of the oxidative reaction limiting the interaction with H_2O_2 at neutral pH. The hydrogen-bonding strength between the TyrB10 and the heme ferryl species suggests the presence of a cycle where the ferryl consumption by the ferric heme increases significantly the pseudoperoxidase activity of these hemeproteins.

Keywords Tyrosine B10 · Ferryl species · Hydrogen peroxide · *Lucina pectinata* hemoglobins · Proximal HisF8 *trans* effect

W. De Jesús-Bonilla · A. Cruz · A. Lewis · J. López-Garriga (✉)
University of Puerto Rico, Mayagüez Campus,
P.O. Box 9019, 00680-9019 Mayagüez, Puerto Rico
E-mail: sonw@caribe.net
Fax: +1-787-2655476

D. E. Bacelo
School of Science and Technology, Universidad Metropolitana,
P.O. Box 21150, 00928-1150 San Juan, Puerto Rico

C. L. Cadilla
Department of Biochemistry, School of Medicine,
University of Puerto Rico, P.O. Box 365067,
00936-5067 San Juan, Puerto Rico

J. Cerda
School of Medicine, University of Pennsylvania,
Philadelphia, PA 19104-6059, USA

Introduction

Cell-free hemoglobins have been considered as hemoglobin substitutes, but oxidative reactions significantly affect their stability [1]; thus, the reaction between hemoglobin and H_2O_2 is one of the most used to elucidate hemeprotein oxidative modifications, because peroxidation affects oxygen binding and heme redox reactions. This reaction produces a high-valence iron species, porphyrin π-cation radical ferryl compound I (Fe^{IV} = O $Por^{\bullet+}$), which can spontaneously decay to its one-electron reduction product, called ferryl compound II (Fe^{IV} = O Por) [2–4]. Nagababu et al. [5] have proposed that when H_2O_2 is present in excess, heme distortion from tetragonal toward rhombic symmetry and loss of the porphyrin iron [6] occurs. Moreover, the reactions of superoxide anions and H_2O_2 dismutation species with proteins are detrimental in red cell pathological conditions. Other studies with human hemoglobin HbA_0 conjugated to carboxylate dextran (Dex-BTC-Hb) have indicated, in part, that the autoxidation and redox reactions with H_2O_2 [7] are insensitive to changes in pH. This indicates that polarity, charge,

pH, and heme pocket distal and proximal environment can affect the reaction of a hemeprotein and H_2O_2. The findings also suggest that in the reaction of these hemoglobins, the formation of compound I occurs via a radical mechanism and that the distal histidine may enhance the decay of compound I to compound II [8].

Previous studies of the reaction of *Lucina pectinata* hemoglobin I (HbI) with H_2O_2 showed a stable and characteristic band for ferryl compound I at 648 nm, attributed to the unusual collection of amino acids (GlnE7, PheB10, PheCD1, PheE11) present in the heme pocket [9]. Stopped-flow analysis of the 648-nm band showed that the oxidation rate of the ferric heme is 2.0×10^{2} M^{-1} s^{-1} and the decay of HbI compound I to compound II is 3.0×10^{-2} s^{-1}. Studies of His64Ala, His64Ser, and His64Leu myoglobin (Mb) variants with *m*-choloroperbenzoic acid [10] assigned the presence of a 648-nm band to Mb compound I. These spectral bands are similar to those reported by Alayash et al. [11] in the reaction of Mb variants with H_2O_2. Native Mb [12] showed the formation of Mb compound I on a 50-ms time scale. In comparison, the presence of the 648-nm band in HbI demonstrated the ability of this hemoglobin to stabilize ferryl compound I. The stability of this band and the resulting reaction kinetics support our hypothesis that the initial formation of the 648-nm band corresponds to the ferryl intermediate HbI compound I, while the Soret band at 419 nm, and the other absorption bands at 539 and 580 nm involve the ferryl species HbI compound II. The presence of longer-lasting bands at 648, 419 and 580 nm suggests that the distal amino acids (GlnE7, PheB10, PheCD1, PheE11) in the heme pocket stabilize the HbI compound I and compound II species [9, 13].

Resonance Raman analysis of the reaction between deoxyHbI and H_2O_2 indicated that both the *trans*-ligand effect and the polarizabilty of the HbI heme pocket are responsible for the observed ferryl oxo vibrational mode at 805 cm^{-1} [13]. Ferryl oxoMb showed a frequency at 797 cm^{-1}, which is higher compared with that of the same mode (779 cm^{-1}) of horseradish peroxidase [14], and cytochrome *c* oxidase [15] and cytochrome *bo* [16] at 785 and 783 cm^{-1}, respectively. Structurally, factors that influence these ferryl oxo stretching frequencies are the polarity of heme pocket residues, the electron donating/withdrawing character of the porphyrin, in addition to steric and hydrogen-bonding interactions [17], while for deoxyHbI and deoxyMb, the Fe–His normal mode appears at 218.5 and 220 cm^{-1}, respectively [18]. The trend between these frequencies is similar to that for other hemeproteins and suggests that the *trans*-ligand effects of the Fe–HisF8 moiety also contribute to determine the observed HbI ferryl oxo frequency. Thus, to unravel the environmental factors that determine the behavior of HbI compound I and compound II it is necessary to establish the contribution of the proximal *trans*-ligand strength, local protein pocket polarizability, and distal hydrogen-bonding effects to the individual heme ferryl species.

Similar to elephant and shark Mb [19, 20], the three hemoglobins of *L. pectinata* [21] have a glutamine (GlnE7) in the distal position instead of a histidine, but they also have phenylalanine in the E11 and CD1 positions. However, in the B10 position, HbI has a phenylalanine residue, while hemoglobin II (HbII) and hemoglobin III (HbIII) have a tyrosine. The HbII oxygen association rate ($k_{on}=0.4\times10^{-6}$ M^{-1} s^{-1}) is between 250 and 500 times smaller than that of HbI ($k_{on}=100$–200×10^{-6} M^{-1} s^{-1}) and is among the lowest known. The HbII oxygen dissociation rate ($k_{off}=0.11$ s^{-1}) is approximately 500 times slower than the HbI dissociation rate ($k_{off}=61.1$ s^{-1}). These findings suggest that stabilization of the oxygenated structure of HbII may be due to multiple hydrogen-bonding interactions. Moreover, the presence bands of the A_3 and A_o conformers at 1,924 and 1,964 cm^{-1} in the HbIICO IR spectra confirms the existence of open and closed conformations due to the orientation of the TyrB10 with respect to the heme active center. In the open conformation, the TyrB10 swings away from the iron, while in the closed conformation, it interacts with the heme ligand moiety [22].

Here, we used UV–vis spectroscopy to study the pH dependence of the reaction kinetics between native HbII, recombinant HbI, and the B10(Tyr) HbI site-directed mutant and H_2O_2, as well as resonance Raman scattering analysis of deoxyHbI and deoxyHbII. Our results show that the kinetics constants for the reaction of recombinant HbI, HbII, and HbI PheB10Tyr mutant with H_2O_2 decrease as a function of increasing pH, which indicates that hydrogen bonding by the B10 tyrosine controls the formation and decay of compound I to compound II ferryl species. At the same time, this decay of heme ferryl compound I is independent of the proximal *trans*-ligand strength.

Materials and methods

Hemeproteins separation and purification

L. pectinata HbII was isolated and purified from the complex with HbIII as described previously [23, 24]. Briefly, a HiLoad 26/60 Superdex 200 grade (ÄKTA FPLC, Amersham Bioscience) column was used to isolate the protein samples. The column was equilibrated to pH 7.5 with 0.5 mM EDTA and 50 mM sodium phosphate buffer at a flow rate of 4.4 ml min^{-1} and 0.5 mPa and the protein concentrations in each fraction was determined from the absorbance at 280 nm. The HbII and HbIII proteins were isolated and purified from the HbII/HbIII fraction by ion-exchange chromatography with a HiPrep 16/10 Q FF column equilibrated with 10 mM triethanolamine/acetate buffer at pH 8.3 and eluted with a gradient of sodium chloride concentration from 0 to 180 mM. Sample purity was determined by sodium dodecyl sulfate polyacrylamide gel electrophoresis. HbII ferric species were prepared by oxidizing the

ferrous HbII with potassium ferricyanide followed by an Amicon ultrafiltration with YM 10 membranes to remove unreacted ferricyanide. Hemeprotein concentration was determined using the extinction coefficient of the ferrous and ferric species [19]. The sample pH was controlled using a buffer solution of 0.1 N *N*-(2-hydroxyethyl)piperazine-*N*′-propanesulfonic acid (HEPES), and HbII alkaline solutions were prepared using a 0.1 N tris(hydroxymethyl)aminomethane (Tris) base buffer solution at pH 11.5.

Recombinant HbI and HbI PheB10Tyr mutant proteins were prepared in a large-scale expression process using a 5-l BioFlo 3000 Fermentor (New Brunswick) with slight modifications [23-25]. The reddish-brown pellets were lysed by five cycles of sonication with 10 ml of Tris–EDTA buffer (10 mM Tris–HCl, 0.1 mM EDTA, pH of 8.0) for every 50 ml of culture. The purification of the expressed hemeproteins was achieved in three steps: First, the lysate was added to a metal-affinity resin (Talon, Invitrogen) and washed with buffer (50 mM Na_2HPO_4, 0.3 M NaCl and 10 mM imidazole, pH 7.6). After the last wash, 15–20 ml (for each 5 ml of resin) of buffer (50 mM Na_2HPO_4, 0.3 M NaCl, 150 mM imidazole, pH 7.6) was used to elute the protein. The imidazole and salts were removed with a High Trap desalting column and the hemeprotein final purification was achieved by fast protein liquid chromatography–size-exclusion chromatography with a Sephadex G-25 column using the native binding buffer (58 mM Na_2HPO_4, 17 mM NaH_2PO_4, 0.3 M NaCl, pH 7.5). The ferric form of the HbI PheB10Tyr mutant, at pH 4.86, was prepared from the reduced species using a buffer solution of 0.1 N HEPES containing 10% of potassium ferricyanide. Excess ferricyanide was removed by ultrafiltration and the pH was adjusted as describe before.

pH dependence of the reactions of hemoglobins with H_2O_2

Recombinant HbI and HbI PheB10Tyr mutant acid–base titration was measured from 700 to 325 nm, at intervals of 0.2 nm, using a double-beam Shimadzu UV–vis instrument (UV-2101 PC). The hemoglobin sample (1 ml, 18 μM) was placed in a quartz cell and the pH was determined with a Beckman 32 pH meter equipped with a microelectrode (Wilmad 6030-02 BNC pH electrode), when the initial UV–vis spectrum was acquired. The acid and basic titration consisted of addition of 0.5 μl of acid or base (0.1 M HCl for the acid titration and 0.1 M NaOH for the base titration) to the sample under stirring for 45 s, followed by the acquisition of the UV–vis data. The volume of the acid or base solution was varied if the change in pH was less than 1.5 units, and this sequence was repeated until the pH of the sample was approximately 11 and approximately 3 for the base and acid titrations, respectively. Before starting the second titration for each hemoglobin sample, the pH was adjusted to the same value as for the first titration to ensure identical initial conditions. The Specfit/32 software (Spectrum Software Associates, Chapel Hill, NC, USA) was use for the 3D and 2D data representations.

Kinetics of the reactions of hemoglobins with H_2O_2

Kinetics experiments were performed using a rapid-scanning monochromator (Olis) with a stopped-flow apparatus. Recombinant HbI, HbII and HbI PheB10Tyr mutant were mixed with H_2O_2 in ratios from 1:100 to 1:6,500. The formation of ferryl compounds I and II were monitored at 400 and 540, and 648 nm, at 22 °C over periods ranging from 1 to 10 s at 5-ms intervals. The pH dependence for the ferryl derivatives of the hemeproteins was followed at acid (pH 4.86), neutral (pH 7.5) and alkaline (pH 11.2) pH. The rate constants at each H_2O_2 concentration were calculated based on the mechanism (Fig. 1) used for HbI [9, 13, 26, 27], where the observable kinetics constants from the biphasic raw data set at 400 and 648 nm were calculated using single value decomposition, global analysis, and curve-fitting routines included in the Olis software. The reversible reactions of the heme compound II with H_2O_2 were not monitored or included for corrections in this study. Since the absorbance maintains proportionality to concentration, the equation that describes the peroxidative reaction of hemeproteins for the global analysis and curve fitting was

$$A_t = \alpha e^{-k_1 \mathrm{obs} \times t} + \beta e^{-k_2 \mathrm{obs} \times t}. \quad (1)$$

The sum of the observable kinetics constants k_1^{obs} and k_2^{obs} in the overall reaction was defined as

$$k_1^{\mathrm{obs}} + k_2^{\mathrm{obs}} = \left(k'_{12} + k'_{21} + k'_{13} + k'_{31}\right)[\mathrm{H_2O_2}] + k_{23}. \quad (2)$$

The slope of the graph of $k_1^{\mathrm{obs}} + k_2^{\mathrm{obs}}$ versus the H_2O_2 concentration in Eq. 2 gives the sum of k'_{12}, k'_{21}, k'_{13}, and k'_{31}. The behavior of the 648-nm band represents the oxidation of the heme Fe(III) to ferryl compound I and the decay of compound I to compound II. The former

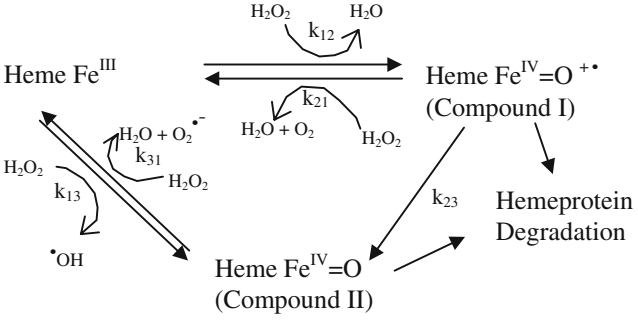

Fig. 1 Mechanism used to define the kinetics constants for the reaction between met aquo recombinant hemoglobin I (*HbI*), hemoglobin II (*HbII*) and HbI PheB10Tyr mutant with H_2O_2

reaction is dependent on the H_2O_2 concentration, while the latter is considered to be independent (k_2^{obs}) of the H_2O_2 concentration. The same approximation holds for the disappearance of the 400-nm band used to follow the presence of compound II. Moreover, since the met aquo hemeprotein derivatives were not observed at the end of the reaction period, k'_{21} and k'_{31} may be assumed to be negligible when they are compared with k'_{12}, k'_{13}, and k_{23} [9, 13] and Eq. 2 is reduced to

$$k_1^{obs} = \left(k'_{12} + k'_{13}\right)[H_2O_2] \text{ and } k_2^{obs} = k_{23}. \quad (3)$$

Resonance Raman scattering data were obtained for deoxy recombinant HbI and HbII. The hemoglobin concentration in each preparation was approximately 100 μM. The spectra were obtained with a 437.0-nm dye laser, pumped with an Ar^+ ion laser (Coherent Innova 400). A back-illuminated CCD detector coupled to a modified Spex 1401 single monochromator and notch filters were used to record the resonance Raman spectra. The monochromator calibration was verified before and after the Raman scattering with carbon tetrachloride. All hemoglobin solutions were spun during the acquisition of the resonance Raman spectra to minimize photoinduced damage to the samples. Laser power was near 10 mW at the sample and each spectrum was averaged for 15 min. A visible spectrum (from 400 to 700 nm) was obtained before and after the resonance Raman measurement to verify sample integrity.

Molecular modeling studies

An initial structure for modeling the active site was prepared from the Protein Data Bank coordinates (1EBT) by adding hydrogen atoms and eliminating amino acids far from the active site. The active-site structure is large and contains 181 atoms. It consists of the porphyrin plane with Fe in the center, the proximal histidine (HisF8) below the plane and four amino acids above, PheB10, PheCD1, PheE11 and GlnE7. Density functional theoretical (DFT) energy evaluations and optimizations were done with the Dmol^3 program [28, 29]. The BPW91 density functional, consisting of Becke's [30] exchange energy functional and the correlation energy functional [31], was employed. The basis sets employed were numerical sets of double numerical plus polarization (DNP) quality. During optimization, the Fe atom with the four nitrogen atoms in the porphyrin, and the proximal histidine, together with H_2O_2 and the atoms of the distal glutamine (GlnE7) were free to float. All other atoms were fixed at their crystallographically determined positions.

Results

The reaction of HbI PheB10Tyr mutant species with a large excess of H_2O_2 is shown in Fig. 2. The spectra

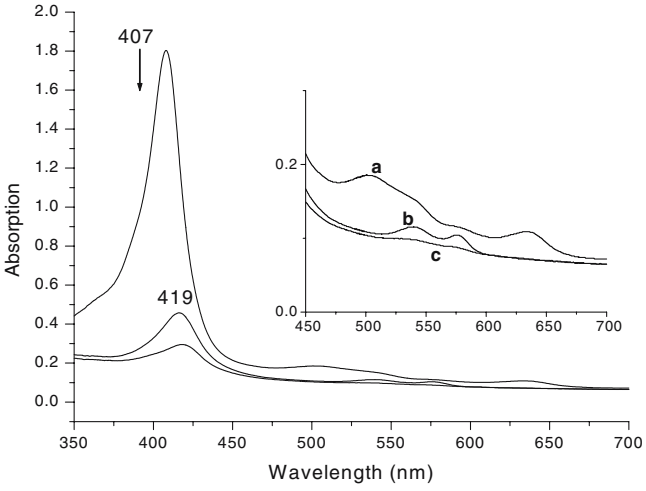

Fig. 2 Reaction of ferric HbI PheB10Tyr mutant in 0.1 M sodium phosphate buffer, pH7, with a large excess of H_2O_2: *a* Unreacted HbI PheB10Tyr; *b* HbI PheB10Tyr after 2 min; *c* HbI PheB10Tyr after 3 min. The *arrow* indicates the decrease in absorption of the Soret band

illustrate that the reaction does not show the formation of the 648-nm band, which is characteristic of the ferryl compound I. In addition, the reactions produce both heme loss and protein degradation, as in wild-type HbI [9]. The same pattern was observed for the reaction of wild-type HbII with different concentrations of H_2O_2. One difference between the HbII and the HbI PheB10Tyr mutant is that the reaction is faster for the former than for the latter. The inset in Fig. 2 shows that for HbI PheB10Tyr mutant the Q bands characteristic of the ferryl species are still present at 2 min, and degradation occurs 8 min after H_2O_2 addition. A similar trend was observed for the reaction with HbII and H_2O_2, where the bands were significantly reduced (not shown). The data suggest that the TyrB10 orientation and the volume of the heme pocket play a distinctive role in the ferryl formation of the hemeproteins. Figure 3 shows that upon reaction of ferric HbII with H_2O_2 at 1:400 ratios, pH 5, the Soret band at 407 nm decreased in intensity and shifted to 416 nm with an isobestic point at 419 nm. This new spectrum may represent a mixture of the ferryl compound II and the ferrous species [13]. Identical behavior was also observed at pH 5, 7 and 11 for the HbI PheB10Tyr mutant. Figure 4 shows, however, that at pH 7, HbII clearly shifted the Soret band from 407 to 419 nm. This formation of the new band was accompanied by an increase in absorption. These results indicated that, up to 10 s, there is no hemeprotein degradation, while the isobestic point at 416 nm suggests the presence of a new heme species. The increase in intensity of the absorbance at 419 nm indicates differences in the molar extinction coefficient, which were attributed to changes in spin from met aquo ferric heme to the ferryl oxo low-spin derivatives.

Figure 5 presents the behavior of the second-order rate constant, as a function of pH, for the formation of the ferryl species in the reactions between HbII and HbI

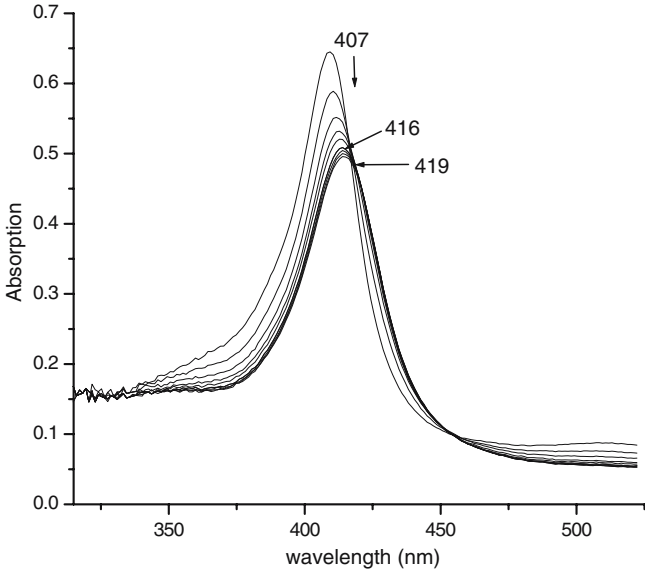

Fig. 3 Reaction of ferric HbII or HbI PheB10Tyr with H_2O_2 at 1:400 ratio in 0.1 N *N*-(2-hydroxyethyl)piperazine-*N*′-ethanesulfonic acid buffer solution (pH 5). After 5 s, the ferric moiety (first spectrum) shifts from 407 to 416 nm with an isobestic point at 419 nm

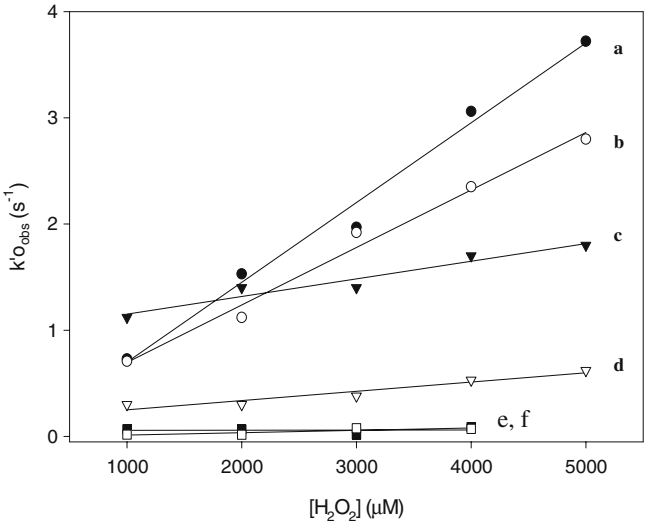

Fig. 5 Rate constants for the reaction between H_2O_2 and *a* HbII at pH 5, 141 M^{-1} s^{-1}, *b* HbI PheB10Tyr mutant at pH 5.0, 103 $M^{-1}s^{-1}$, *c* HbII at pH 7.5, 78 M^{-1} s^{-1}, *d* HbI PheB10Tyr mutant at pH 7.5, 69 M^{-1} s^{-1}, *e* HbII at pH 11.2, 3.0 M^{-1} s^{-1}, and *f* HbI PheB10Tyr mutant at pH 11.2, 1.5 M^{-1} s^{-1}. Hemoglobins were reacted with H_2O_2 in ratios from 1:100 to 1:6,500. The formation of the ferryl compound I and compound II was monitored at 400, 540, and 648 nm, at 5-ms intervals and over periods ranging from 1 to 10 s

PheB10Tyr mutant with H_2O_2. Upon changing the pH from 5 to 7.5 (Fig. 5, spectra a and b and spectra c and d, respectively) there is a significant decrease in both the k_{obs} values and the slope of the plot, related to the second-order rate constant for the reaction. A further decrease in the rate constant is observed at pH 11.2 (Fig. 5, spectra e and f). Also, within the same pH, there are differences between the kinetics of the reaction between HbII and HbI PheB10Tyr mutant with H_2O_2. At pH 5, the rate constants are 141 and 103 M^{-1} s^{-1}, respectively, while at pH 7.5, these constants decrease to 78 and 69 M^{-1} s^{-1}, and at pH 11.2 there is a further decrease to 3.0 and 1.5 M^{-1} s^{-1}. In all cases, the difference in the rate constant values can be explained by changes in the heme coordination and ligation state during the titration of met HbII and met aquo HbI PheB10Tyr mutant.

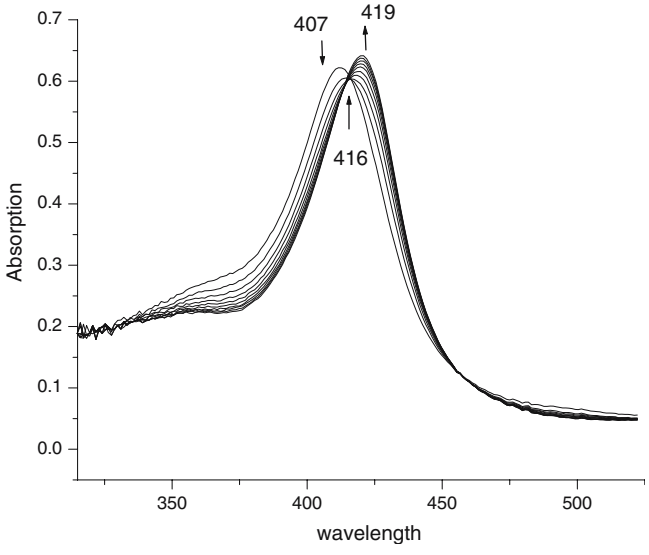

Fig. 4 Reaction of ferric HbII in sodium phosphate buffer with H_2O_2 at 1:400 ratio at a neutral pH (7.4). The Soret band shifts from 407 to 419 nm with an isobestic point at 416 nm. *Upward* and *downward arrows* indicate changes in the extinction coefficient

Figure 6 shows how several absorption bands change as a function of pH on decreasing it from 8.0 to 4.0. The inset in Fig. 6 presents a more detailed view of the Q-bands region. The transitions between species are associated with the disappearance of met aquo HbII tyrosinate (486, 541, 577, and 603 nm) and the evolution of met aquo HbII (502 and 630 nm). The pH data supports the presence of heme tyrosinate species during the titration of both hemeprotein samples. However, this pH-dependent behavior is not observed for the reaction between H_2O_2 and HbI [9] and recombinant HbI, which both have a phenylalanine in the B10 position instead of tyrosine.

Figure 7 shows the Q band of the recombinant HbI ferric heme at 633 nm, which in the presence of H_2O_2 shifts to 648 nm increasing the absorbance. The kinetics behavior of this band upon reaction of recombinant HbI, pH 7, with H_2O_2 is shown in Fig. 8. The reactions at ratios of 1:100 and 1:250 (Fig. 8, spectra a and b) present an increase in the rate, which reached a plateau between ratios of 1:500 and 1:1,000 (Fig. 8, spectra c and d). At ratios of 1:2,000 to 1:4,000, the rate shows biphasic behavior (Fig. 8, spectra e and f). These results support the idea that TyrB10 ligation to the metallo active center in hemeproteins and the hydrogen bonding

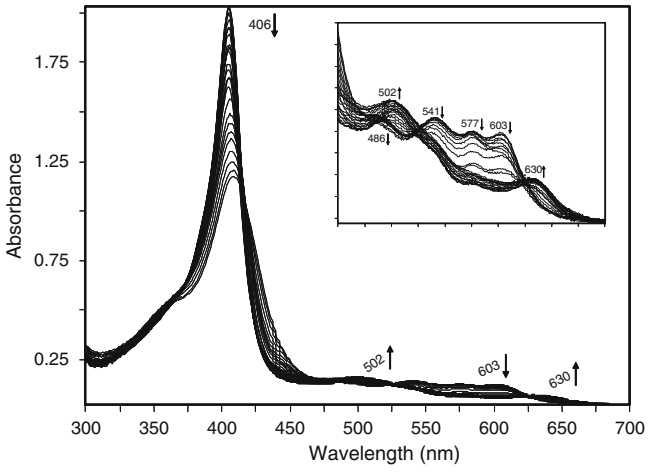

Fig. 6 pH dependence in the formation of tyrosinate species during the titration of met aquo HbII. The *arrows* indicate the behavior of the absorption band as the pH decreased. The *inset* shows the Q-bands region, where the transition between species is associated with the disappearance of metHbII tyrosinate (486, 541, 577 and 603 nm) and the evolution of met aquo HbII (502 and 630 nm)

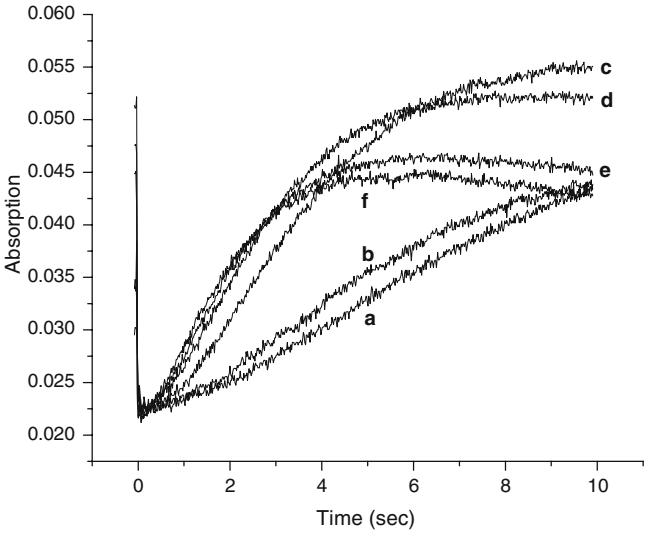

Fig. 8 Time course of the reaction between recombinant HbI (pH 7) and H_2O_2 at 648 nm at ratios of 1:100 (*a*), 1:250 (*b*), 1:500 (*c*), 1:1000 (*d*), 1:2,000 (*e*), and 1:3,000 (*f*). The reactions at ratios of 1:100 and 1:250 present an increase in the rate, which reached a plateau between ratios of 1:500 and 1:1,000

between the ferryl in compound I and the amino acid hydroxyl group play a significant role in defining the presence of the 648-nm band and in the reactivity of ferryl species.

Figure 9 compares the low-frequency resonance Raman spectra of ferrous deoxygenated HbII and recombinant HbI samples, which give information about the Fe–His stretching mode and the *trans* effect of the proximal histidine. Normal-mode assignments were based on the presence or absence of a particular frequency in the resonance Raman spectra for the HbI–ligand complexes and upon comparison of these values with those reported in the literature. The Fe–N (His) stretch has been observed in the resonance Raman spectra of hemoglobins and Mbs in the 217–224-cm^{-1} region [18]. For the recombinant deoxyHbI spectrum the low-frequency region is characterized by a strong band at 218.5 cm^{-1} assigned to the Fe–N_ε stretching mode, which is almost identical to the Fe–N_ε frequency of Mb at 220 cm^{-1}. However, for HbII Fe–N_ε this mode is present at a relatively lower vibrational frequency of 210 cm^{-1}, suggesting that the proximal HisF8 *trans* effect is not the same for both proteins. When both spectra are compared, they reveal

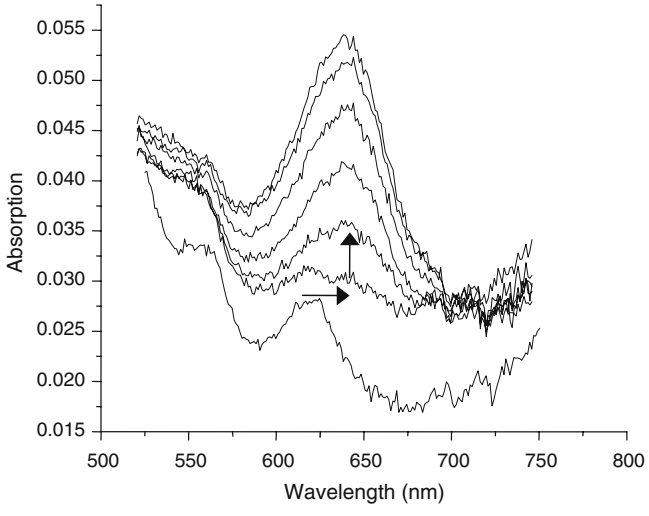

Fig. 7 Reaction for 10 s of recombinant met aquo HbI (pH 7) with H_2O_2 (1:2,000) at 648 nm. The *horizontal arrow* indicates a shift from 633 nm, at 1 s the band shifts to 648 nm, whereas the *vertical arrow* indicates increases in the presence of compound I

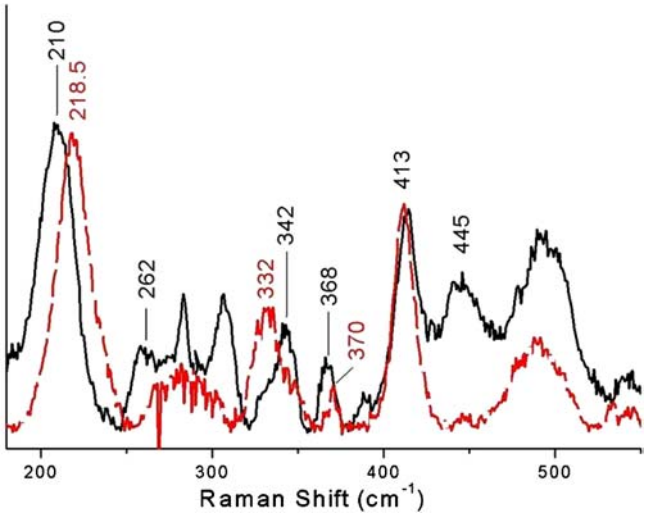

Fig. 9 Resonance Raman scattering was obtained for deoxy recombinant HbI (*dashed line*) and HbII (*solid line*). The hemoglobin concentration in each preparation was approximately 100 μM. The spectra were obtained with 437.0-nm excitation

differences in the 260–280, 325–350, 365– 380, and 440–500 cm^{-1} regions. In the recombinant HbI the 270-cm^{-1} band was assigned to the skeletal mode ν_9. The band at 332 cm^{-1} is assigned to ν_8, to a metal pyrrole stretch and substituent bend. For HbII, this mode appears at higher frequency, 342 cm^{-1}, and is due to the out-of-plane pyrrole-tilting mode. The data also show that there is no significant difference for recombinant HbI and HbII, with a band at 370 cm^{-1}, attributed to C_β–C_c–C_d bending motion of the peripheral heme substituents of the propionates, with the exception that for recombinant HbI this band appears with lower intensity than for HbII.

Discussion

pH dependence of hemeprotein reactions with H_2O_2

Kraus and Wittenberg [21] reported a low pK_a for the acid–alkaline transition of HbII and HbIII from *L. pectinata*. In the acid derivative, a water molecule is present in the distal side interacting with the iron and the distal amino acids, while in the alkaline analog, the TyrB10 and hydroxide ion interact with the heme. This interaction was evident by comparison of the electron paramagnetic resonance data of HbII and HbIII with other hemeproteins suggesting the existence of two different species in the alkaline structure [21, 32]. Thus, it is possible to monitor the interaction of TyrB10 in HbII and HbI PheB10Tyr mutant by pH titration as observed in *Chlamydomonas* hemoglobin and *Scapharca* hemoglobin [32–35]. Therefore, the results presented in Fig. 6 showed that met aquo HbII exists alone at acidic pH, typically absorbing at 630 nm, while at neutral pH there is a mixture of species related to the HbII heme–tyrosinate moiety and the met aquo HbII derivatives, 603 and 630 nm, respectively [22]. Similarly, Fig. 10 indicates that the titration of the HbI mutant shows almost the same behavior of the 603-nm band, which is attributed to a TyrB10 interaction with the heme iron. For this interaction to occur, the tyrosine residue needs to be very close to the heme iron, thus providing an optimal distance for the interaction. However, for the HbI PheB10Tyr mutant, the interaction of the TyrB10 is evident from pH > 6 and does not disappear at higher pH, indicating that there are stronger contacts than in HbII. The pH profile suggests that the tyrosine residue has to be nearest to the heme Fe(III) moiety in both proteins to provide the optimal distance for the interaction of the TyrB10 with the heme active center.

The data presented in Table 1 clearly show that for HbII and the HbI PheB10Tyr mutant both the pH and the presence of the heme–tyrosine interaction decreased the observed ferryl species, thus suggesting a faster cycle of H_2O_2 consumption by the ferric species. It can be inferred that at low pH the incoming H_2O_2 displaced the water molecule in the hemeprotein Fe(III) center, and

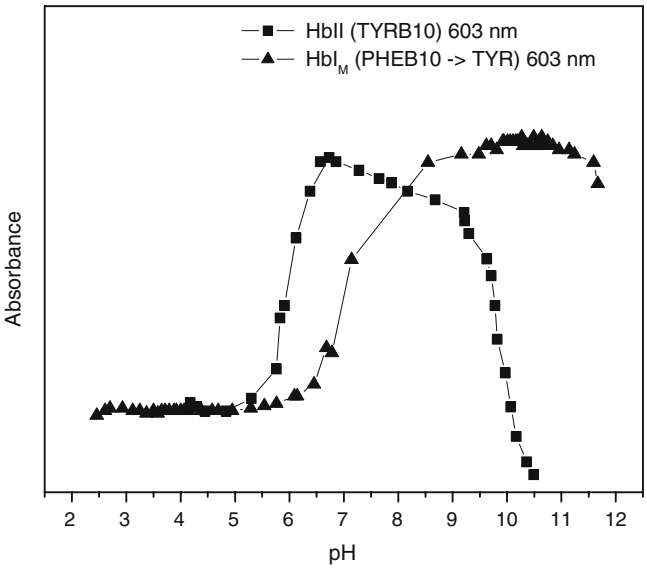

Fig. 10 Titration of the 603-nm band for HbII (*squares*) and HbI PheB10Tyr mutant (*triangles*) as function of pH

the complex was stabilized by hydrogen bonding with TyrB10. At neutral pH, the met aquo heme complex is in equilibrium with the iron–tyrosine moiety and the concentration of hemoglobin available to react with H_2O_2 is lower, with the concurrent decrease in the second-order rate constant. At alkaline pH, the strong interaction between the heme Fe(III) and the OH ligand further decreased the rate constant because of the presence of the heme Fe(IV) = O compound. This trend is similar to that shown to exist in previous work on the reaction of Mb with H_2O_2 [6, 8, 36, 37]. Even though the rate constants for the formation of compound II are very similar for HbII and HbI PheB10Tyr mutant (Table 1), their different values are associated with heme cavity differences [22], decreasing the formation rate of the ferryl species, and increasing the decay rate, in the presence of hydrogen bonding, from compound I to compound II. Furthermore, the presence of the A_3 and A_o conformers at 1,924 and 1,964 cm^{-1} in the HbIICO IR spectra confirmed the existence of an open and closed conformation due to the orientation of the TyrB10 with respect to the heme active center. That is, in the open conformation, TyrB10 swings away from the iron, while in the closed conformation, TyrB10 is very close and may interact with the ligand [22]. Thus, the rate constants indicated that the rate for the formation of the ferryl intermediates varied with pH (Table 1), suggesting

Table 1 Kinetics constants for hemoglobin II (*HbII*) and hemoglobin I (*HbI*) mutant with H_2O_2 at 400 nm

pH	HbII (M^{-1} s^{-1})	HbI PheB10Tyr (M^{-1} s^{-1})
5.0	141.60	103.45
7.5	77.79	69.00
11.2	2.96	1.56

also that the reaction is also strongly dependent on the conformation of the amino acid that may interact with the heme ferryl species.

Role of TyrB10 and HisF8 *trans* effect in the ferryl transition from compound I to compound II

Figure 1 shows the catalytic cycle of ferric hemeproteins [9, 13, 26, 27], where the reaction of the heme Fe(III) species with peroxide produces an intermediate, compound I, which contains a heme Fe(IV) = O ferryl cation radical [38]. The first step in the reaction is believed to be the formation of an Fe(III)–peroxo species [39, 40], which undergoes very rapid heterolytic O–O bond cleavage, assisted by the conserved distal histidine [41]. Moreover, mutants lacking this distal histidine display decreased activity toward the formation of compound I [42, 43]. Stopped-flow measurements of ferric HbI from *L. pectinata* have shown [9] that the rate constant for the conversion of compound I to compound II is 3.0×10^{-2} s^{-1}, which is more than 100 times smaller than that reported for Mb [13]. At the same time the rate constant for the HbI ferryl formation at pH 7.5 is 2.0×10^{2} M^{-1} s^{-1}, which is similar to the values of 6.6×10^{2} and 6.7×10^{2} M^{-1} s^{-1} for Mb variants [6] His64Gln/Leu29Phe Mb and sperm whale Mb [12]. In these cases a large k_{12} (Fig. 1) implies a high H_2O_2 consumption rate in the peroxidative cycle. The HbI distal pocket has a Gln64, and three phenylalanine groups (PheB10, PheCD1, PheE11) and the orientation in GlnE7 allows the possible formation of a carbonyl–H_2O_2–heme moiety that precedes the HbI formation of compound I and compound II, respectively. To examine the possibility of this heme–peroxide complex as a prelude to oxidation we performed a DFT optimization of H_2O_2 at the HbI active site. Figure 11 displays an optimized BPW91 DFT structure that confirms the formation of a stable initial complex between peroxide and the active site. The presence of this intermediate agrees with early proposed models for the reaction between Mb and H_2O_2 [44, 45]. The calculated geometry suggests that the incoming H_2O_2 is held in place by hydrogen-bonding interactions with the carbonyl group of GlnE7 (1.78 Å in length) and with one of the pyrrole nitrogens (N–H distance 2.13 Å) in the heme, while the distance from Fe to the nearest peroxide O is 2.89 Å. The binding strains H_2O_2; its dihedral angle (132°) is more than 20° more open than in the isolated molecule.

Independent of the structural changes associated with the heterolytic O–O bond cleavage, resonance Raman studies demonstrate the formation of both met aquo HbI and compound II ferryl species in the cyclic reaction of HbI with H_2O_2. The compound II ferryl vibration frequency appears at 805 cm^{-1} for $HbIFe^{IV}=O$ species. Our data support the hypothesis that the CO of GlnE7 is ultimately oriented toward the heme–peroxide moiety, limiting the presence of hydrogen bonding between the transient ferryl intermediates and the nearby amino acids. A direct implication of

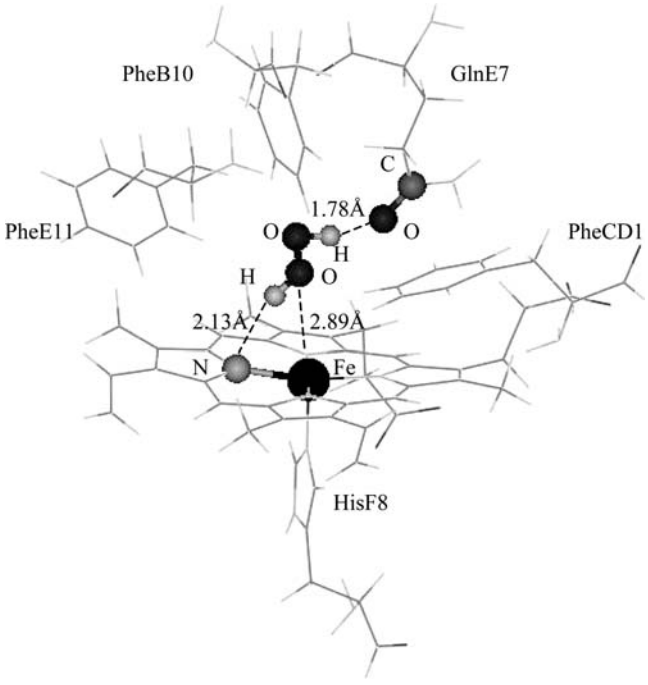

Fig. 11 Optimized BPW91/double numerical plus polarization structure of the initial complex between HbI and H_2O_2

this structural state is the presence of the 648-nm transition associated with an extended lifetime of compound I in the HbI [9] and recombinant HbI species (Fig. 7). The similar kinetics of the 648-nm band in the recombinant HbI and HbI wild type upon reaction with H_2O_2 strongly suggest that amino acids in the E7 and B10 positions have an important role in the control of the rate constants k_{12} and k_{23} (Fig. 1), which lead to the formation of the ferryl species, compounds I and II. Moreover, substitution of PheB10 by tyrosine in the HbI PheB10Tyr mutant or in HbII produces, upon reaction with H_2O_2, a spectroscopic pattern, similar to Mb [1], which lacks the 648-nm intermediate. The finding that the ligand interaction with glutamine stabilizes the H_2O_2 adduct is not new [9–13]. Previous studies with Mb showed similar networking between the ferryl porphyrin radical and the amino acids tryptophan and tyrosine [46, 47]. The 648-nm band represents the formation and autoreduction of HbI compound I. However, our study complements previous studies by adding specific kinetics analysis involving the band at 648 nm and a hydrogen-bonding mechanism for the decay of compound I to compound II. The kinetics constant k_{23} (Fig. 1) for the decay of HbI from compound I to compound II (Eq. 3), is $3.0\pm0.02\times10^{-2}$ s^{-1}, which is similar to that for the recombinant HbI and is 100 times faster than the rate constant reported for Mb, 4.0 s^{-1} [9]. These observations support a model where the strength of hydrogen bonding between TyrB10 and compound I increases the ferric–ferryl cycle avoiding the accumulation of ferryl species.

Importantly, compound I decay is the limiting step in the formation of compound II ferryl species, and a lower k_{23} suggests that H_2O_2 contributes to the stability of both compound I and the ferric HbI state. However, in HbII and HbI PheB10Tyr mutant, the interplay of TyrB10 conformations creates a hydrogen-bond network that neutralizes very quickly compound I, absence of the 648-nm transition in the spectra, leading to an increase in k_{23} and rapid formation of compound II. The rate constant k_{23} (Fig. 1) has to be higher than the added value of the other rate constants ($k_{12}^{'} + k_{13}^{'}$) for the formation of compound II. The fine-tuning for these rate constants depends on the electrostatic interactions between the ferryl chromophore and the heme pocket amino acids. In this regard, an intense band at 218.5 cm^{-1}, characterizes the Fe–N_ε stretching mode for both HbI and recombinant HbI, while for HbII this mode is present at a relatively lower vibrational frequency of 210 cm^{-1}. At the same time, reaction of both ferric proteins with H_2O_2 indicates that the band at 648 nm is present in the spectra of HbI and recombinant HbI, but it is absent for HbII and the HbI PheB10Tyr mutant. Moreover, the Fe–N_ε stretching mode for the HbI mutant is present at a higher energy (220 cm^{-1}) (unpublished results). Since both HbII and HbI PheB10Tyr mutant have a TyrB10 but differ in the Fe–N_ε mode at 210 and 220 cm^{-1}, respectively, the decay of the ferryl compound I to compound II must be independent of the HisF8 *trans* effect. Moreover, the presence of hydrogen bonding between the ferryl moiety and heme pocket amino acids not only controls the decay of these species (k_{23} in Fig. 1) but also suggests the presence of a cycle where the ferryl consumption by the ferric heme increases significantly the pseudoperoxidase activity of these hemeproteins.

Acknowledgements This work was supported in part by funds from NIH (COBREIP20RR016439), NIH (SCORE506GM08103-27), UPR and the Alfred P. Sloan Foundation (UPR-Mayagüez).

References

1. Yeh LH, Alayash AI (2003) J Intern Med 253: 518–526
2. Schöneboom C, Neese F, Thiel W (2005) J Am Chem Soc 127: 5840–5853
3. Cashon RE, Alayash AI (1995) Arch Biochem Biophys 316: 461–469
4. Whitburn KD (1987) Arch Biochem Biophys 253: 419–430
5. Nagababu E, Ramasamy S, Rifkind JM (2002) Biochemistry 41: 7407–7415
6. Alayash AI, Brockner Ryan BA, Eich RF, Olson JS, Cashon RE (1999) J Biol Chem 274:2029–2037
7. Jia Y, Wood F, Menu P, Faivre B0, Caron A, Alayash I (2004) Biochim Biophys Acta 1672:164–173
8. Kato S, Ueno T, Fukuzumi S, Watanabe Y (2004) J Biol Chem 279:52376–52381
9. De Jesús-Bonilla W, Cortés-Figueroa JE, Souto-Bachiller FA, Rodríguez L, López-Garriga J. (2001) Arch Biochem Biophys 390: 304–308
10. Matsui T, Ozaki S, Watanabe Y (1997) J Biol Chem 272: 32735–32738
11. Alayash AI, Ryan BA, Eich RF, Olson JS, Cashon RE (1999) J Biol Chem 274:2029–2037
12. Egawa T, Shimada H, Ishimura Y (2000) J Biol Chem 275:34858–34866
13. De Jesús-Bonilla W, Ramirez-Melendez E, Cerda J, López-Garriga J (2002) Biopolymers 67:178–185
14. Sitter AJ, Reczek CM, Terner J (1985) Biochim Biophys Acta 828:229–235
15. Varotsis C, Babcock GT (1990) Biochemistry 29:7357–7362
16. Uchida T, Mogi T, Kitawaga T (2000) Biochemistry 39:6669–6678
17. Oertling WA, Kean R, Wever R, Babcock GT (1990) Inorg Chem 29:2633–2645
18. Cerda J, Echevarría Y, Morales E, López-Garriga J (1999) Biospectroscopy 5:289–301
19. Romero-Herrera AE, Goodman M, Dene H, Bartnicki DE, Mizukami H (1981) J Mol Evol 17: 140–147
20. Suzuki T, Suzuki T, Yata T (1985) Aust J Biol Sci 38: 347–354
21. Kraus DW, Wittenberg JB (1990) J Biol Chem 265:16043–16053
22. Pietri R, Granell L, Cruz A, De Jesús W, Lewis A, León RG, Cadilla CL, López-Garriga J (2005) Biochim Biophys Acta 1747:195–203
23. León RG, Munier-Lehmann H, Barzu O, Baudin Creuza V, Pietri R, López-Garriga J, Cadilla CL (2004) Protein Expr Purif 38:184–95
24. Navarro A, Maldonado M, González-Lagoa J, López-Mejías R, Colón J, López-Garriga J (1996) Inorg Chim Acta 243:161–166
25. Collazo E, Pietri R, De Jesús W, Ramos C, Del Toro A, León RG, Cadilla CL, López-Garriga J (2004) Protein J 23:239–245
26. Matsui T, Ozaki S, Liong E, Phillips GN, Watanabe Y (1999) J Biol Chem 274:2838–2844
27. Nagababu E, Rifkind JM (2000) Biochemistry 39:12503–12511
28. Delley B (1990) J Phys Chem 92:508–517
29. Delley B (2000) J Chem Phys 113:7756–7764
30. Becke AD (1988) J Chem Phys 88:1053–1062
31. Lee C, Yang W, Parr RG (1988) Phys Rev 37:785–789
32. Das KT, Boffi A, Chiancone E, Rousseau AD (1999) J Biol Chem 274:2916–2919
33. Das KT, Franzen S, Pond A, Dawson HJ (1999) Inorg Chem 38:1952–1953
34. Das K, Couture M, Lee HC, Peisach J, Rousseau LD, Wittenberg BA, Wittenberg JB, Guertin M (1999) Biochemistry 38:15360–15368
35. Lukat-Rodgers SG, Rexine LJ (1998) Biochemistry 37:13543–13552
36. Reeder BJ, Svistunenko DA, Sharpe MA, Wilson MT (2002) Biochemistry 41:367–375
37. Newmyer SL, Ortiz de Montellano PR (1995) J Biol Chem 270: 19430–19438
38. Bosshard HR, Anni H, Yonetani T (1990) In: Everse J, Everse KE, Grisham MB (eds) Peroxidases in chemistry and biology, vol II. CRC Press, Boca Raton, pp 51–84
39. Miller MA, Shaw A, Kraut (1994) J Struct Biol 1:524–531
40. Poulos TL, Kraut J (1980) J Biol Chem 255:8199–8205
41. Finzel BC, Poulos TL, Kraut J (1984) J Biol Chem 259:13027–13036
42. Erman JE, Vitello LB, Miller MA, Shaw A, Brown KA, Kraut (1993) J Biochemistry 32:9798–9806
43. Palamakumbura AH, Vitello LB, Erman JE (1999) Biochemistry 38:15653–15658
44. Nilsson K, hersleth HP, Rod TH, Andersson KK, Ryde U (2004) Biophys J 87:3437–3447
45. Egawa T, Yoshioka S, Takahashi S, Hori H, Nagano S, Shimada H, Ishimori K, Morishima I, Suematsu M, Ishimura Y (2003) J Biol Chem 278:41597–41606
46. DeGray JA, Gunther MR, Tschirret-Guth R, Ortiz de Montellano PR, Mason RP (1997) J Biol Chem 272:2359–2362
47. Østdal H, Søgaard SG, Bendixen E, Andersen HJ (2001) Free Rad Res 35:757–766